18TH WORLD CONFERENCE ON EARTHQUAKE ENGINEERING
WCEE2024
MILAN

MILAN, ITALY
30TH JUNE - 5TH JULY 2024
www.wcee2024.it

ASSESSMENT OF MASONRY TOWERS SEISMIC VULNERABILITY THROUGH NON-LINEAR SSI NUMERICAL MODELLING

A. di Lernia[1], A.F. D'Oria[1], G. Uva[1] & G. Elia[1]

[1] DICATECh – Technical University of Bari, Bari, Italy (annamaria.dilernia@poliba.it)

Abstract: *The paper investigates the role of soil-structure interaction (SSI) phenomena on the seismic vulnerability of ancient masonry towers through a 3D non-linear finite element approach. The investigation is conducted considering an ideal masonry tower, representative of many recurring bell towers located in the seismic areas of northern Italy, resting on deformable heterogeneous soil deposits, whose dynamic features cover the typical lithological successions of clays and sands in Italy. The masonry behaviour is described throughout a plastic-damage constitutive model, while a linear and an equivalent-linear visco-elastic approach is adopted for the soil. After preliminary modal eigenvalues analyses aimed at identifying the natural frequency of the linear SSI system, complete three-dimensional non-linear dynamic analyses are carried out to assess the tower seismic vulnerability. Additionally, a set of decoupled analyses, consisting in the implementation of the fixed-base structural scheme subjected to the seismic input motion accounting for both the seismic site response and the kinematic interaction of the structure-foundation system, is also considered to highlight the influence of the soil compliance on the structural response. The numerical results are discussed in terms of damage distributions and structural displacements recorded along the structure in elevation. The study suggests that the SSI can clearly affect the seismic performance of ancient masonry towers, modifying the modal properties, the seismic demand and the possible collapse modes affecting the structure if compared to the fixed-base scheme.*

1. Introduction

The assessment of the seismic performance of masonry towers has recently become a central topic in structural engineering. Indeed, masonry towers are widespread in many European countries, representing one of the most prominent portions of our cultural and historical legacy. At the same time, this kind of structures is often characterized by a high seismic vulnerability depending on some peculiar features. Structural slenderness and geometrical irregularities, e.g., vaults, inclination of the structure and openings on the façade (especially close to the belfry), are some of the main aspects that can affect the dynamic response of towers (Bartoli et al., 2017; Casolo et al., 2013; Ferrante et al., 2019; Valente and Milani 2018, 2016). Furthermore, the material properties along with the type of masonry texture represent other relevant key points controlling the mechanical behaviour and the failure mechanisms exhibited by the masonry structures (Bartoli et al., 2013; Vasconcelos and Lourenço, 2009).

The analysis of the structural behaviour is typically performed assuming a perfectly fixed-base condition (e.g., Acito et al., 2014; Bayraktar et al., 2018; Castellazzi et al., 2017). However, this assumption is not always suitable to represent the actual in-situ soil conditions, as the foundation deposits can be also characterized by soft soils sequences that should not allow to use this approximation. Indeed, soil deformability can considerably modify the dynamic behaviour of a structure, since its response during a seismic event is the result of the

mutual interaction between the structure itself, the supporting foundation and the surrounding soil, commonly known as dynamic soil-structure interaction (SSI). Nonetheless, the effect of soil compliance is still just occasionally considered, despite the location of a tower on deformable soil deposits, which also typically correspond to areas subjected to severe seismic hazard levels, is not so remote, as reported by de Silva et al. (2015) for some of the main Italian towers.

Most of the relevant studies found in the literature considered a homogeneous soil deposit below the tower and focused on the role played by the seismic input motion characteristics on the dynamic response of the structure (Mortezaei and Motaghi, 2016; Casolo and Uva, 2013). In Casolo et al. (2017), the damage pattern induced in the tower was also related to the modal shape changes due to the soil deformability. In de Silva (2020), a set of idealized masonry towers having no irregularities and different slenderness ratios were studied throughout non-linear dynamic analyses, considering various homogeneous soil deposits characterized by an equivalent-linear visco-elastic behaviour. A realistic soil stratigraphic profile is, instead, rarely considered in the simulations, except for very few cases (de Silva et al., 2018; Somma et al., 2023).

Within this context, the present study aims at assessing the SSI effects on the seismic vulnerability of an ideal masonry tower resting on heterogenous soil deposits by means of 3D non-linear simulations. The work covers two main aspects of the problem: the role played by the soil deposit conditions in terms of soil stratigraphic heterogeneity and the impact of the soil non-linearity, adopting a linear visco-elastic (LIN) and an equivalent-linear visco-elastic (EQ-LIN) model to simulate the soil dynamic response. The mechanical behaviour of the masonry material is described through an advanced constitutive model accounting for a plastic-damage behaviour.

2. Description of the case study and numerical models

The tower structural model herein considered refers to the ideal case study outlined by Casolo et al. (2017), which embodies the main features of many recurring bell towers located in the seismic areas of northern Italy. The 3D finite element (FE) model adopted in the simulations is shown in Figure 1a, implementing the ideal tower, supposed to be structurally independent from other buildings, resting on a heterogeneous 30m thick soil deposit. The simulations have been conducted using the commercial code Abaqus (2014). The geometrical configuration of the tower is regular both in plan and in elevation, with a square base section of 5.30m x 5.30m, a larger square foundation of 6.80m x 6.80m and total height of 27m, resulting in a slenderness ratio equal to 5. The masonry walls thickness starts from 1.0m at the base and then it reduces to 0.85m at the top. The tower has been assumed to rest on ideal heterogeneous soil deposits, characterized by different stratigraphic sequencies, whose shear wave velocity (V_S) profiles cover the range identified by Falcone et al. (2021) for typical lithological successions of clay and sand cover soils in Italy, as described in D'Oria et al. (2022).

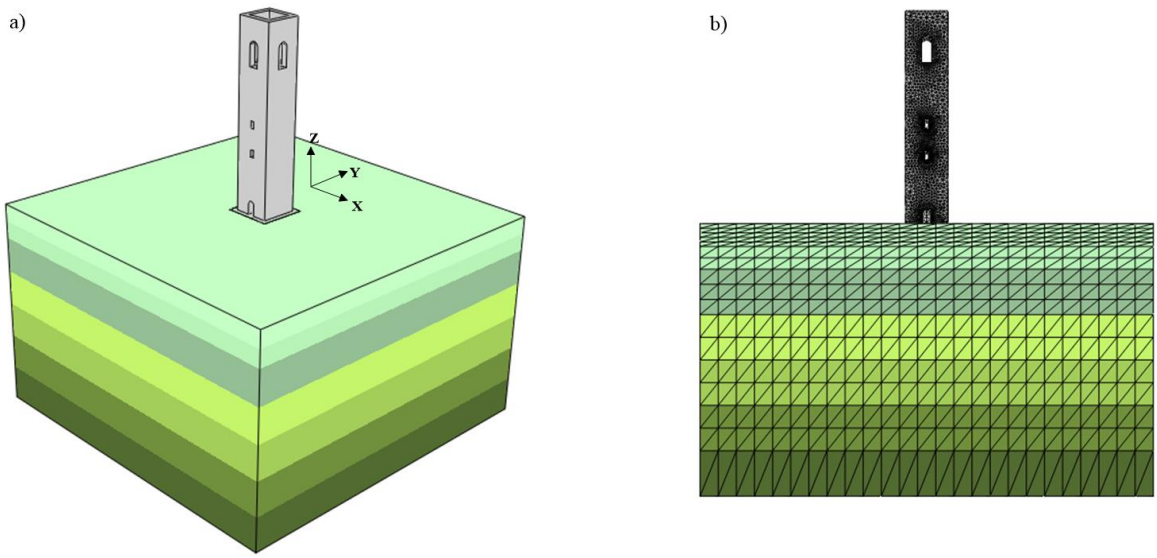

Figure 1. a) 3D numerical model and b) FE mesh adopted in the simulations with Abaqus.

Seven deformable soil deposits resting on a bedrock layer (characterized by V_S greater than 800 m/s) have been considered in this investigation. Figure 2a shows the adopted V_S profiles with depth, which share the same value of the equivalent shear wave velocity $V_{S,eq}$ equal to 250 m/s, defined as:

$$V_{S,eq} = \frac{H}{\sum_{i=1}^{N} \frac{h_i}{V_{S,i}}} \quad (1)$$

where N is the number of the layers, h_i is the thickness of the i-th layer, $V_{S,i}$ is the shear wave velocity of the i-th layer, while H is the deposit depth, equal to 30m. Thus, according to the Italian Code NTC2018 (Consiglio dei Ministri, 2018), the soil deposits can be classified as class C, i.e. characterized by a $V_{S,eq}$ between 180 and 360m/s. The soil stratigraphies shown in Figure 2 can be divided into two groups. The first one is composed by multiple soil layers deposits classified by means of the heterogeneity parameter α (Vinale and Simonelli, 1983), defined as:

$$\alpha = \frac{V_H}{V_0} \quad (2)$$

where V_H and V_0 are the shear wave velocity at the bottom and at the surface of the soil deposit, respectively. Five different values of α have been considered in the simulations: a value of 1, corresponding to a homogeneous condition, and the values of 2.5, 5, 10 and 15. The second group is, instead, composed by simpler two-layered soil deposits, representative of a clay over sand (CS in Figure 2) and a sand over clay (SC in Figure 2) sequence, with the aim of investigating the effect of a shear wave velocity inversion. The CS deposit is characterized by a heterogeneity parameter equal to 2.28, while α is equal to 0.44 in the SC case. The profiles of the initial shear stiffness modulus G_0 corresponding to the V_S profiles shown in Figure 2a are reported in Figure 2b.

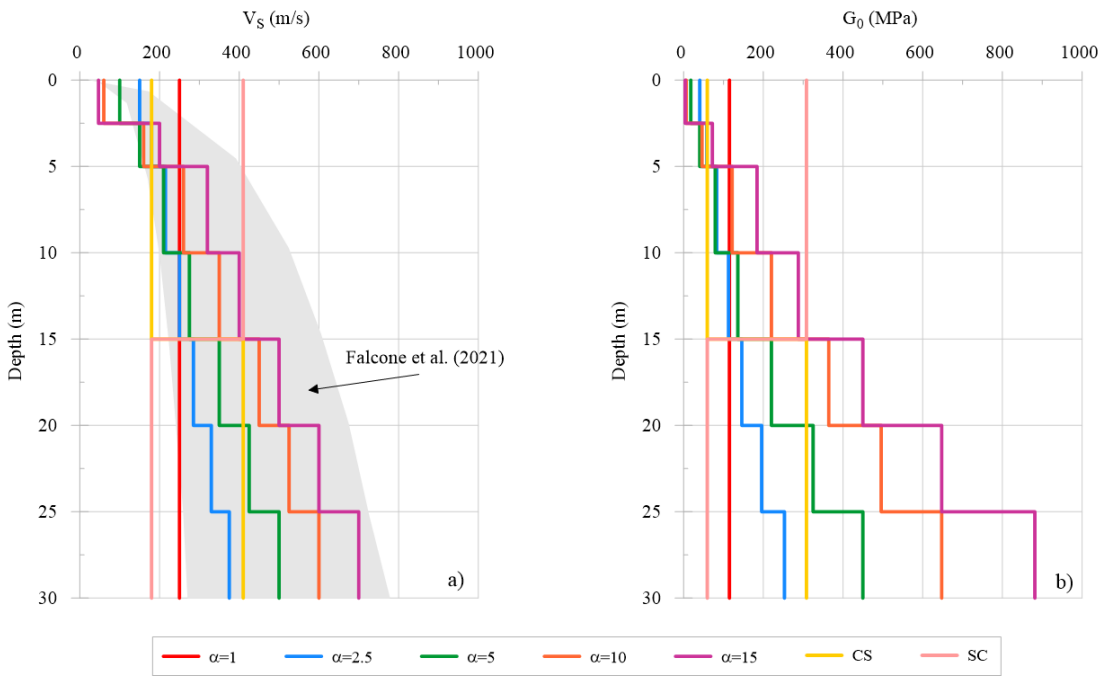

Figure 2. a) shear wave velocity V_S and b) initial shear stiffness G_0 soil profiles corresponding to different values of the heterogeneity parameter α.

The 3D FE mesh of the soil deposit (Figure 1b), discretized using 4-node linear tetrahedral elements (C3D4), has a height of 30m and a width of 50m along each horizontal direction, in order to prevent from any boundary effect on the structural response. Moreover, the coarseness of the FE mesh of the soil domain has been refined to obtain a distance between two consecutive nodes smaller than approximately one-eighth of the wavelength associated with the maximum frequency content of the input motion (Bathe, 1996), set equal to 15Hz. In

addition, since each soil profile is characterized by rather different V_S values, the mesh refinements of the soil domains have been optimized case by case in order verify the above-mentioned requirement. Finally, the mesh of the tower has been refined around the openings and close to the base, in order to achieve an adequate numerical accuracy, resulting in total number of nodes equal to 21547. The interface between the foundation and the deposit has been realized with a master-slave relationship: a penalty-type interaction law has been defined for the tangential behaviour, while a hard-contact type law has been imposed in the normal direction to prevent the interpenetration between the contact surfaces.

To avoid spurious wave reflections at the vertical boundaries of soil deposit model, the so-called “tied-nodes” boundary condition, which ensures that the nodes located on the left and right sides of the soil domain exhibit the same displacements, has been employed. The modal frequency analyses have been performed adopting the Lanczos method (Grimes et al., 1994), while the dynamic analyses have been carried out using the unconditionally stable implicit Hilber-Hughes-Taylor time integration scheme (Hilber and Hughes, 1978), which ensures the stability of the algorithm without introducing any additional numerical damping.

The reference input motion employed in the numerical simulations is represented by the X component of the South Iceland earthquake occurred on the 17th of June 2000, recorded on a class A site. The seismic signal is characterized by a maximum acceleration of 0.12g, a predominant frequency around 4.2Hz and a time step acquisition equal to 0.005s. The acceleration time history of the input motion has been directly applied to the rigid base of the 3D model.

The mechanical behaviour of the masonry tower has been described by the Concrete Damaged Plasticity (CDP) model (Lubliner et al., 1989; Lee and Fenves, 1998), implemented in the material model library of Abaqus. Although the CDP model was originally conceived for isotropic fragile materials, like concrete, it has been adapted and successfully used in a wide number of masonry applications (Acito et al., 2014; Tiberti et al., 2016; Karimi et al., 2016; Castellazzi et al., 2017). The model accounts for a scalar isotropic damage with distinct damage parameters under tensile and compression loading conditions. Therefore, it is particularly suitable for masonry behaviour since this material exhibit asymmetry in terms of both damage and strength in tension and compression, especially in loading-unloading conditions, such as those associated to seismic loading. A summary of the CDP parameters and the mechanical properties adopted for the ideal masonry tower is reported in Table 1.

Table 1. CDP model parameters adopted for the masonry tower.

ρ (Kg/m^3)	E_0 (MPa)	ν	ψ (°)	f_{b0}/f_{c0}	ε	K_c
1900	3500	0.1	20	1.16	0.1	2/3

The response of the soil deposits has been modelled adopting the linear visco-elastic approach (LIN), to evaluate the solely influence of the stratigraphic heterogeneity, whereas the equivalent-linear visco-elastic (EQ-LIN) model has been used to account for soil non-linearity. When the LIN approach is adopted, the shear stiffness profiles implemented in the FE models are those corresponding to the initial shear stiffness G_0 shown in Figure 2b. When the soil non-linearity is also accounted for, a preliminary seismic response analysis is required to determine the soil dynamic parameters varying with depth associated to the shear strain level induced by the specific input motion. In this latter approach, preliminary 1D site response analyses have been performed in the frequency domain through the equivalent-linear visco-elastic code EERA (Bardet et al., 2000), by implementing the shear modulus decay curve and the variation of damping ratio D with shear strain level proposed by Vucetic and Dobry (1991) for a plasticity index equal to 50%. The effect of considering the soil non-linearity is the reduction of the soil resonance frequencies and the attenuation of the predicted PGA, if compared to that obtained through linear visco-elastic analyses. In the equivalent visco-elastic approach, the output results obtained from EERA represent the input for the FE simulations (Amorosi et al., 2010). Hence, each soil layer in the FE model is characterized by the shear modulus G and damping ratio D attained at the end of the seismic action, variable with depth.

The dissipative capacity of the soil has been introduced through the frequency-dependent Rayleigh damping formulation (Rayleigh, 1945). The Rayleigh coefficients α_R and β_R have been derived as a function of the target viscous damping D* according to:

$$\begin{Bmatrix} \alpha_R \\ \beta_R \end{Bmatrix} = \frac{2D^*}{\omega_m + \omega_n} \begin{Bmatrix} \omega_m \omega_n \\ 1 \end{Bmatrix} \quad (3)$$

where the angular frequencies ω_m and ω_n are related to the frequencies f_m and f_n, defining the interval over which the viscous damping is equal to or lower than the target viscous damping ratio D*. The two control frequencies have been set equal to the first and second natural frequency of the soil deposit, since the dynamic behaviour of the tower is particularly influenced by the second natural mode of the soil deposit, as revealed by the modal eigenvalue analyses.

3. Numerical results

3.1 Modal frequency analysis

To assess the influence of soil deformability on the modal properties of the tower, frequency eigenvalues analyses have been performed, comparing the results to the fixed-base scenario (assuming the absence of the soil deposit). Due to the symmetrical geometry characterizing the structure, the flexural modes of the fixed-base structure are specular in X and Y direction, while the torsional mode contribution is very low (about 0.20% of the excited mass). According to the modal analysis, the first and second natural frequency of the fixed-base tower are equal to 1.9Hz and 8.7Hz, respectively.

The first and second natural frequency of the soil-tower systems (i.e., f_{SSI-1} and f_{SSI-2}) and the ratio between these SSI frequencies and the corresponding natural frequencies of the soil deposit (i.e., $\xi_1 = f_{SSI-1}/f_{SOIL-1}$ and $\xi_2 = f_{SSI-2}/f_{SOIL-2}$) are listed in Table 2 for both LIN and EQ-LIN analyses, highlighting how the natural frequencies of the structure on a compliant base are quite variable depending on the stratigraphic heterogeneity. This reflects the frequency variability obtained from the EERA analyses in free-field conditions and confirm the soil compliance relevance.

Independently on the adopted soil modelling approach, a clear reduction in the natural frequencies of the tower standing on deformable soils with respect to the fixed-base condition is recognizable for both the first and second mode of vibration. The SC case present the less significant reduction, probably because it is characterized by the highest value of V_S in the upper part of the deposit (equal to 410 m/s), which makes it closer to a rigid soil condition.

As expected, the non-linear soil effects (EQ-LIN results) produce a further reduction in the structural natural frequencies. Finally, for both LIN and EQ-LIN approaches, the ratios ξ_1 and ξ_2 show that, except for the SC case, f_{SSI-1} is lower and quite distant from f_{SOIL-1}, while f_{SSI-2} can be either higher or smaller than f_{SOIL-2}, but in all cases much closer to f_{SOIL-2}. Therefore, f_{SOIL-2} might affect the dynamic response of the tower as well as yield to SSI resonance phenomena.

Table 2. First and second natural frequency of the tower resting on deformable soil and normalized values considering the corresponding soil resonance frequencies (ξ_1 and ξ_2).

	LIN				EQ-LIN			
SOIL PROFILE	f_{SSI-1} (Hz)	f_{SSI-2} (Hz)	ξ_1	ξ_2	f_{SSI-1} (Hz)	f_{SSI-2} (Hz)	ξ_1	ξ_2
α = 1	1.43	7.41	0.68	1.19	1.27	6.75	0.69	1.19
α = 2.5	1.30	7.67	0.52	1.20	1.04	6.54	0.46	1.11
α = 5	1.15	6.28	0.40	0.95	0.90	5.57	0.33	0.91
α = 10	1.12	6.22	0.33	1.01	0.94	5.55	0.31	1.15
α = 15	1.22	6.52	0.34	1.19	1.12	6.02	0.40	1.25
CS	1.32	7.57	0.53	0.97	1.02	6.73	0.46	1.15
SC	1.68	7.82	1.08	1.28	1.55	6.93	1.13	1.24

The first and second modal shapes of the tower are illustrated in Figure 3 for both LIN and EQ-LIN approaches. To present a more effective comparison with the fixed-base scheme, the displacement profiles have been

depurated from the translational displacements, recorded at the base of the compliant models, and then normalized with respect to the displacements attained at top of the structure for each model. It can be noted that, for both LIN and EQ-LIN soil behaviour, the first modal shape does not seem to be heavily altered by the SSI, as all the structural deformed shapes overlay and are rather close to the fixed-base condition (black line). Conversely, the second modal shape displays a more evident dependence on the soil compliance, consistently with the literature (de Silva et al., 2015; Casolo et al., 2017). Even though a clear trend cannot be identified, it seems that as the soil heterogeneity degree increases, the modal shapes variability reduces. Moreover, the most remarkable changes related to the soil non-linearity effects are restrained to α = 1 and SC cases, for which a higher reduction in the shear stiffness is induced by the earthquake induced strain level. On the other hand, the remaining cases present lower stiffness reductions and, as a result, the second modal shape does not change when the EQ-LIN soil behaviour is adopted.

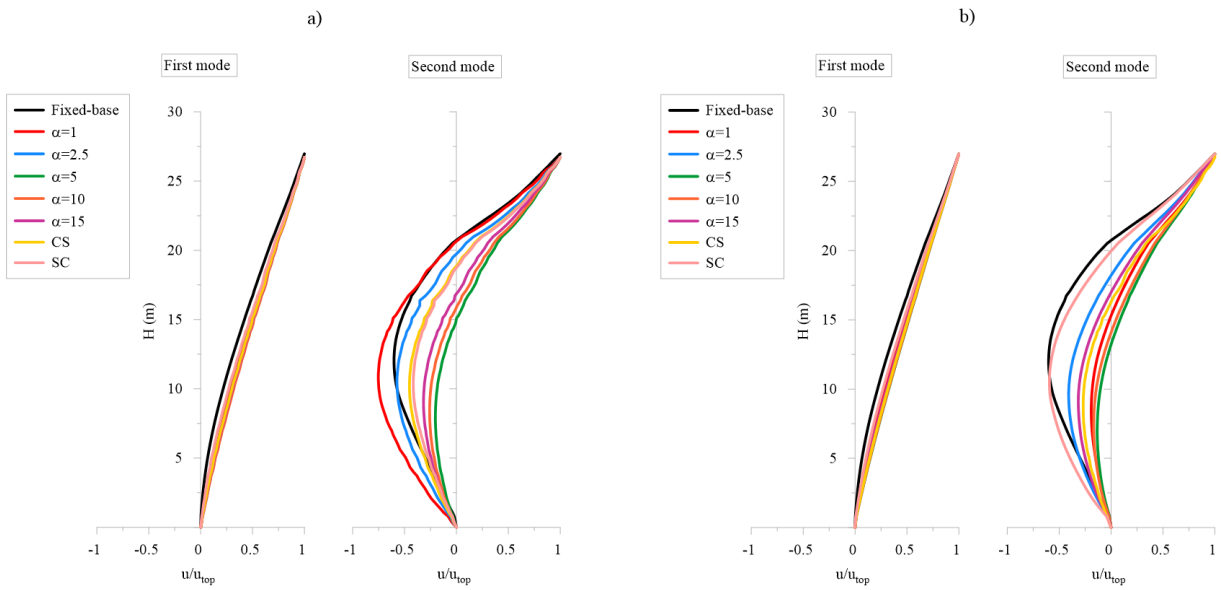

Figure 3. First and second modal shapes in the x direction normalized for the maximum horizontal top displacement: a) LIN and b) EQ-LIN analyses.

3.2 Non-linear time history analyses

To investigate the effect of both soil stratigraphic heterogeneity and non-linearity on the dynamic response of the soil-tower system and, in particular, on the distribution of the damage induced by the seismic action, the non-linear time-history analyses of the 3D soil-tower system were performed adopting the direct approach, consisting in performing a fully coupled analysis of the whole soil-structure system assembled in a finite element (FE) model. As above-mentioned, the CDP model has been used for the masonry tower, while linear visco-elastic and equivalent-linear visco-elastic approaches have been adopted for the description of the soil dynamic parameters. The influence of the interaction between the tower and the compliant soil was evaluated also comparing the fully coupled 3D model results to those derived from a decoupled model, consisting in performing a FE simulation of a cantilever tower subjected, at foundation level, to the motion derived from the SSI analyses. Hence, in both coupled (SSI) and uncoupled (FIX) approaches the structure is subjected to the same signal and all the deviations in the structural response can be related to the inertial interaction phenomena due to the soil compliance.

A synthesis of the tensile damage patterns predicted at the end of the seismic event for all the 3D FE models is shown in Figure 4. The results referring to the linear visco-elastic approach for both SSI and FIX models are reported in Figure 4a, highlighting solely the effect of the stratigraphic heterogeneity on the dynamic response of the tower. The damage distribution can be very different between SSI and FIX models. More specifically, for the homogeneous soil case (α = 1), the SSI simulation appears to produce a more hazardous scenario with respect to the FIX one.

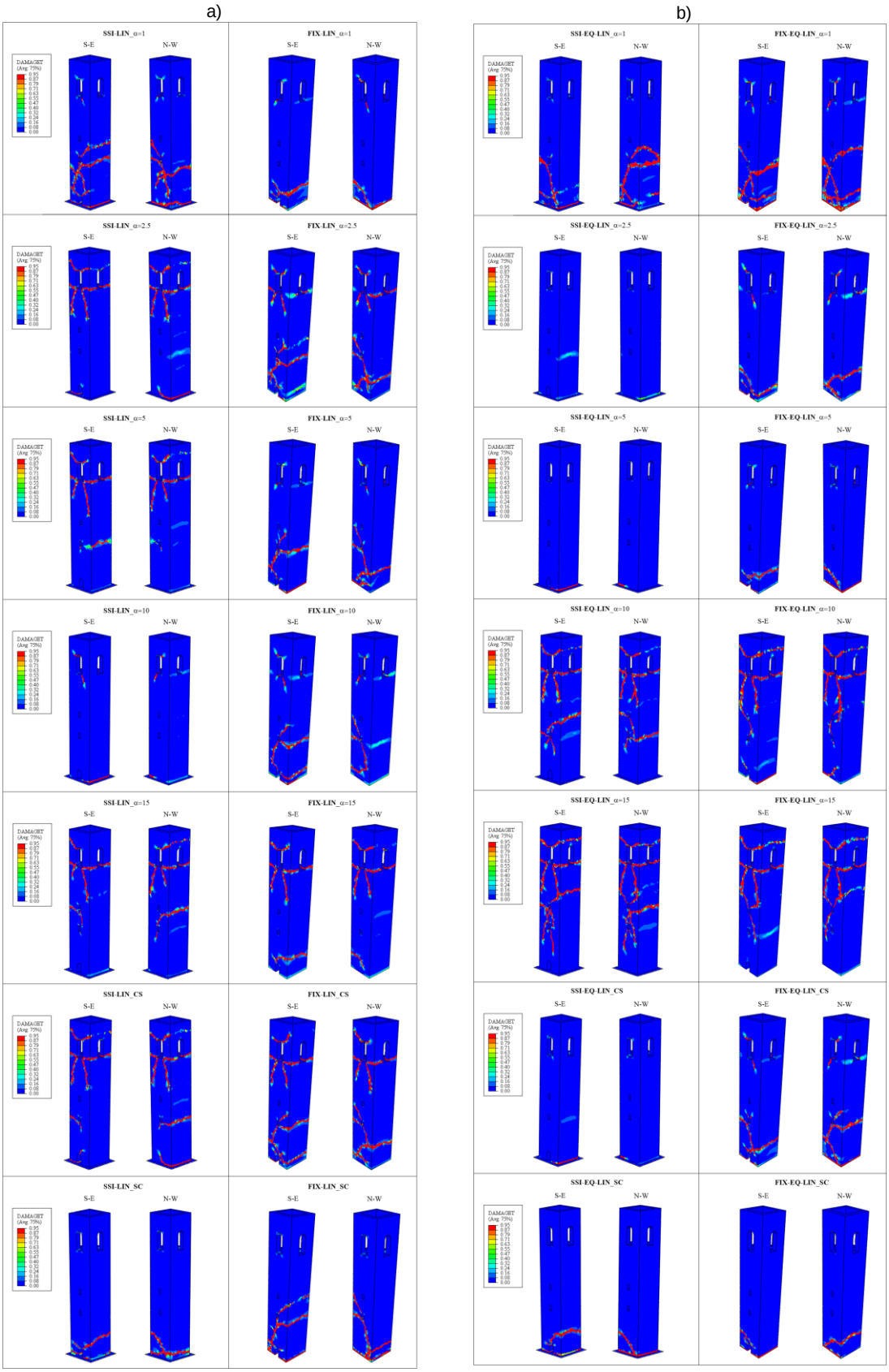

Figure 4. Tensile damage contours at the end of the seismic action for the a) LIN and b) EQ-LIN analyses, compared with the corresponding fixed-base solution.

Indeed, the FIX scheme presents a damage localization close to the basement level of the tower; conversely the SSI model provides a more severe concentration right above the main entrance, characterized by inclined

cracks, and in correspondence of the minor openings in the middle of the structure. In both models, the upper part of the tower is not much affected. In the α = 2.5 case, both schemes are characterized by an evident damage localization in the belfry area, while only in the FIX simulation the first half of the tower results affected by the seismic action. In the α = 5 case, the SSI analysis predicts a damage pattern concentrated at the bell cell, while in the FIX analysis it is localized only right above the main entrance. When α is 10, the SSI analysis provides just very mild damage at the basement level and in correspondence of the upper openings, while the FIX one shows a much more hazardous scenario with diagonal cracks in the first half of the tower and limited material degradation at the belfry. For α = 15, a rather comparable scenario predicted by the two modelling strategies, characterized by a severe damage at the bell cell level, can be observed. In the CS case, the SSI analysis shows that the belfry is once again very affected by the earthquake, while a more limited damage distribution is observed at the basement level and close to the minor openings. Conversely, the FIX analysis manifests severe damage patterns both in the upper and lower part of the structure. Finally, the SC case presents, at least qualitatively, a similar damage scenario for both the fully coupled and the decoupled modelling approach, showing shear diagonal cracks which develop in the first half and at the basement level of the structure.

The tensile damage distributions obtained from the EQ-LIN set of analyses at the end of the seismic event are shown in Figure 4b. In this case, the impact on the damage distribution of soil non-linearity, along with the stratigraphic heterogeneity, is investigated. The α = 1 case is characterized by a rather similar damage scenario for both the SSI and FIX analyses, with clear inclined cracks developing in the first half of the tower and negligible material degradation in the upper part of the structure. On the other hand, the α = 2.5 case presents different patterns depending on the modelling approach adopted. Indeed, the SSI analysis predicts negligible damage along the entire structure, while the FIX analysis provides evident damage concentration right above the main entrance and at the belfry of the tower. The α = 5 case shows low damage levels affecting the structure if the fully coupled approach is considered; conversely, a more demanding damage distribution at the basement level of the tower characterizes the uncoupled analysis. The α = 10 case shows, instead, a comparable damage pattern no matter what model is considered. In fact, the belfry area results very affected by the seismic action in both SSI and FIX models; also, the middle part of the structure presents relevant cracks at minor openings, especially in the SSI case. Conversely, a slight material degradation at the base of the structure can be also recognized only in the FIX case. The α = 15 case provides high damage levels at the bell cell for both modelling approaches; on the other hand, the SSI analysis is characterized by more severe damage distribution in the middle of the tower with respect to the FIX case. The CS case predicts only mild damage at the base of the SSI tower, while more severe cracks distributions are observed in the FIX tower above the main entrance and at the bell cell. Finally, the SC case provides similar damage scenarios in both analyses, predicting damage localization only at the base of the structure.

As a general finding, it can be stated that the soil compliance can potentially affect the damage distribution along the height of the tower, which can be significantly different between the SSI and the FIX models. Important different patterns are, for example, recorded for α = 5 and α = 10 in the LIN set of analyses and for α = 2.5, α = 5 and CS for the EQ-LIN one; in particular, this latter group always show a more limited damage intensity level when the fully coupled approach is considered. Similar trends, instead, can be identified between the SSI and the FIX simulations, as for the α = 15 and SC cases in the LIN set of analyses and α = 1, α = 10 and SC cases for the EQ-LIN one. In addition, for both the LIN and EQ-LIN sets, as the heterogeneity ratio increases the damage distribution looks to affect more often the bell cell, which is known as one of the most sensitive structural parts of ancient masonry towers to earthquakes (Poiani et al., 2018; Ferrante et al., 2019). Anyway, the obtained damage distribution is quite variable from case to case, and it is rather difficult to establish “a-priori” if the soil compliance can produce a significant change of the damage patterns.

In addition, the numerical results have been interpreted in terms of bending and rocking displacements, as defined in Figure 5, where the total horizontal displacement (u_{tot}) of the tower-foundation system is composed by three parts: the translational displacement (u_u), the rocking displacement (u_δ) related to the rotation of the foundation δ and the bending displacement (u_θ) of the structure. Figure 6 shows the comparison between the bending and the rocking displacement time histories obtained at the top control point of the SSI tower for the two soil response assumptions (i.e., LIN and EQ-LIN).

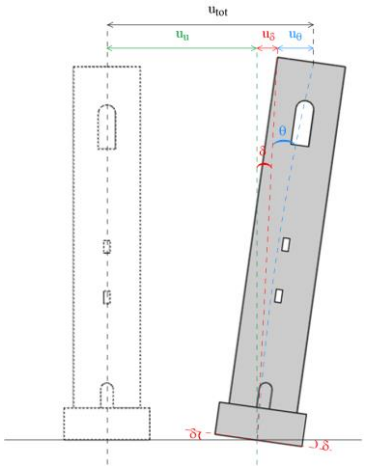

Figure 5. Sketch of the translational (u_u), rocking (u_δ) and bending (u_θ) displacement affecting the tower during the seismic action.

As it can be observed from this figure, the soil behaviour can significantly influence the magnitude and the sign of the accumulated bending displacements, in particular for α = 1, α = 5 and α = 15; conversely, a similar trend is detected for the SC case. Moreover, the introduction of the soil non-linearity through the EQ-LIN approach generally produces higher rocking displacements in each analysed case. This aspect is especially evident in the α = 2.5, α = 5 and CS cases, representing the scenarios in which the tower is less affected by damages at the end of the seismic event. Furthermore, rocking displacements of the order of the bending ones are also recognized for the LIN_ α = 10 analysis, which has shown limited damages. This suggests that the occurrence of consistent rocking motion could mitigate the damage distribution affecting the structure, even though it might cause more hazardous tilts and, hence, instabilities problems.

4. Conclusions

A numerical investigation on the dynamic soil-structure interaction phenomena affecting masonry towers has been presented in this research by comparing fully coupled (SSI) and uncoupled (FIX) approaches. Specifically, the study has mainly focused on two key aspects which can influence the dynamic response of a tower resting on soft soils: the soil stratigraphic conditions and the soil non-linearity. The tower has been described using a plastic-damage model able to catch the main features of the masonry mechanical behaviour, while the dynamic soil behaviour has been simulated using a linear and an equivalent-linear visco-elastic approach.

Preliminary modal eigenvalues analyses showed some of the typical effects of the soil compliance. Indeed, a clear reduction in the natural frequencies of the structure has been recognized. This phenomenon becomes more evident as the soil heterogeneity degree increases and with the adoption of the equivalent-linear formulation for the soil behaviour, usually shifting the seismic demand towards lower spectral accelerations for the first period of oscillation and towards higher values for the second one. Moreover, the first flexural modal shape of the tower appeared not to be sensitive to the interaction phenomena. On the contrary the second mode showed significant changes when a deformable support was considered, as the elongation of the structural periods brings the second frequency of structure to be much closer to the fundamental frequency of the soil.

When conducting non-linear dynamic analyses, the soil-structure interaction can be beneficial or detrimental for the structure, mitigating or enhancing the earthquake effects on the tower, depending on the specific case investigated. Damage patterns and bending displacement plots highlighted different seismic responses of the tower, which are highly dependent on the compliance type and the subsoil characteristics. Hence, the possible failure modes can be remarkably different if soil-structure interaction modelling is considered or not in the structural vulnerability assessment. In addition, the upper part of the tower, including the bell cell, resulted more sensitive to damage if the structure rests on highly heterogenous soil deposits. The introduction of non-linearities in the soil dynamic behaviour causes the increase of the rocking displacement demand. For all these reasons, it is advised to carefully consider the possibility to adequately model the soil domain in the dynamic

simulations, since soil-structure interaction can play a not negligible role on the seismic response of masonry structures.

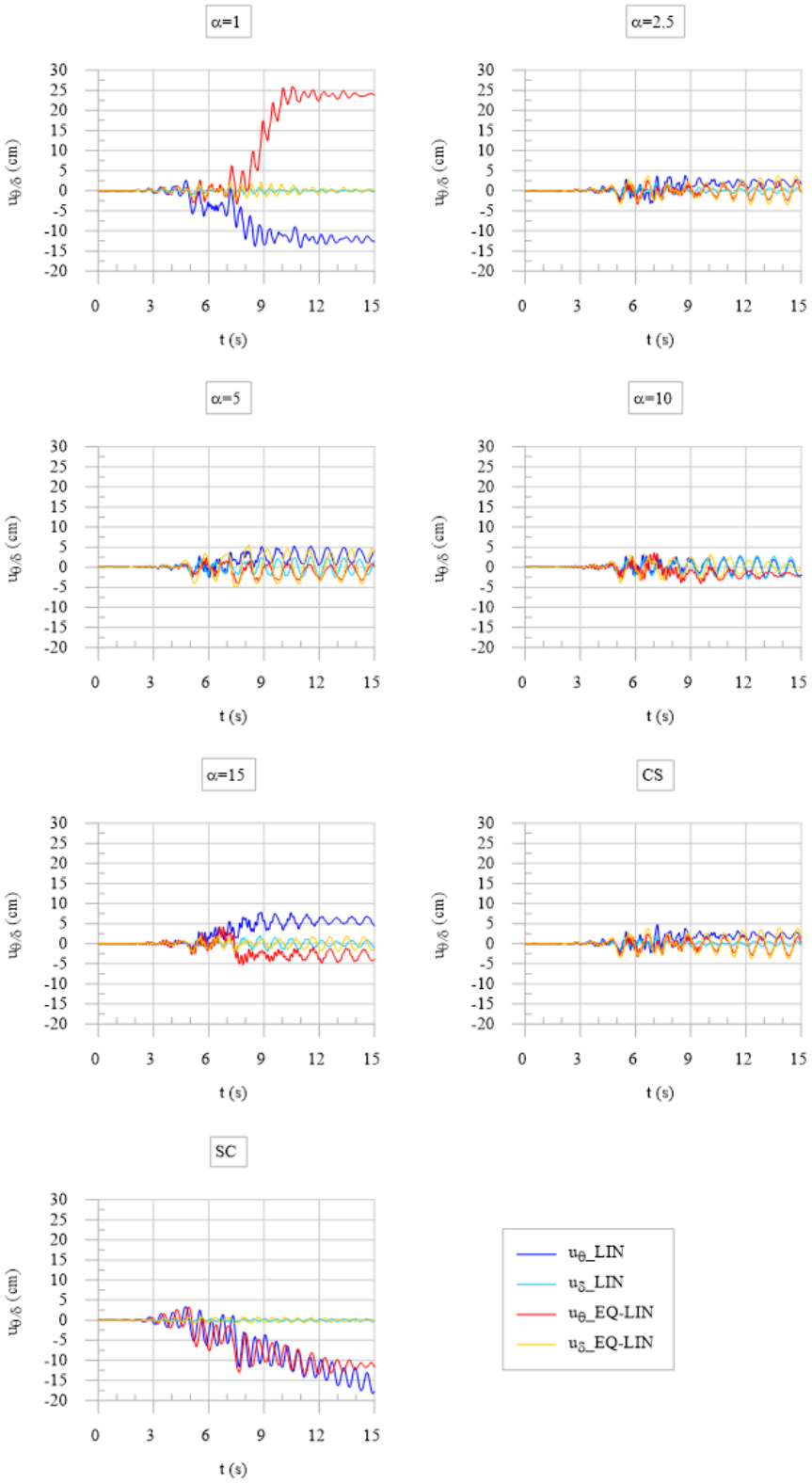

Figure 6. Bending (u_θ) and rocking (u_δ) displacements time-histories recorded at the top of the tower for each LIN and EQ-LIN simulation.

5. References

ABAQUS (2014). ABAQUS documentation version 6.14. Dassault Systèmes, Providence, RI.

Acito M., Bocciarelli M., Chesi C., Milani G. (2014). Collapse of the clock tower in Finale Emilia after the May 2012 Emilia Romagna earthquake sequence: Numerical insight. *Engineering Structures*, 72, 70-91.

Amorosi A., Boldini D., Elia G. (2010). Parametric study on seismic ground response by finite element modelling. *Computers and Geotechnics,* 37, 515–528.

Bardet J.P., Ichii K., Lin C.H. (2000). EERA: A computer program for equivalent-linear earthquake site response analyses of layered soil deposits.

Bartoli G., Betti M., Giordano S. (2013). In situ static and dynamic investigations on the "Torre Grossa" masonry tower. *Engineering Structures*, 52, 718-733.

Bartoli G., Betti M., Monchetti S. (2017). Seismic risk assessment of historic masonry towers: comparison of four case studies. *Journal of Performance of Constructed Facilities*, 31(5).

Bathe K.J. (1996). *Finite Element Procedures*, 2nd ed. Prentice Hall, Upper Saddle River, N.J.

Bayraktar A., Hökelekli E., Halifeoğlu F. M., Mosallam A., Karadeniz H. (2018). Vertical strong ground motion effects on seismic damage propagations of historical masonry rectangular minarets. *Engineering Failure Analysis*, 91, 115-128.

Casolo S., Uva G. (2013). Non-linear dynamic analysis of masonry towers under natural accelerograms accounting for soil-structure interaction. *Proceedings of 4th EC-COMAS, Thematic Conference on Computational Methods in Structural Dynamics and Earthquake Engineering*. Crete, Greece, 4488–4506.

Casolo S., Milani G., Uva G., Alessandri C. (2013). Comparative seismic vulnerability analysis on ten masonry towers in the coastal Po Valley in Italy. *Engineering Structures*, 49, 465-490.

Casolo S., Diana V., Uva G. (2017). Influence of soil deformability on the seismic response of a masonry tower. *Bulletin of Earthquake Engineering*, 15(5), 1991-2014.

Castellazzi G., D'Altri A. M., de Miranda S., Ubertini F. (2017). An innovative numerical modeling strategy for the structural analysis of historical monumental buildings. *Engineering Structures*, 132, 229-248.

Consiglio dei Ministri. (2018). *DM 17 gennaio 2018 in materia di "aggiornamento delle norme tecniche per le costruzioni"*. Gazzetta ufficiale n.42 del 20 febbraio 2018.

de Silva F., Ceroni F., Sica S., Pecce M. R., Silvestri F. (2015). Effects of soil-foundation-structure interaction on the seismic behavior of monumental towers: the case study of the Carmine Bell Tower in Naples. *Italian Geotechnical Journal*, 49(3), 7-27.

de Silva F., Ceroni F., Sica S., Silvestri F. (2018). Non-linear analysis of the Carmine bell tower under seismic actions accounting for soil–foundation–structure interaction. *Bulletin of Earthquake Engineering*, 16(7), 2775-2808.

de Silva F. (2020). Influence of soil-structure interaction on the site-specific seismic demand to masonry towers. *Soil Dynamics and Earthquake Engineering,* 131, 106023.

D'Oria A.F., Elia G., di Lernia A., Uva G. (2022). Influence of soil deposit heterogeneity on the dynamic behaviour of masonry towers. *Proceedings of the 3rd International Symposium on Geotechnical Engineering for the Preservation of Momenuments and Historic Sites (TC301 - IS Napoli 2022).* Naples, Italy.

Falcone G., Acunzo G., Mendicelli A., Mori F., Naso G., Peronace E., Porchia A., Romagnoli G., Tarquini E., Moscatelli M. (2021). Seismic amplification maps of Italy based on site-specific microzonation dataset and one-dimensional numerical approach. Engineering Geology, 289, 106170.

Ferrante A., Clementi F., Milani G. (2019). Dynamic behavior of an inclined existing masonry tower in Italy. *Frontiers in Built Environment*, 5, 33.

Grimes R. G., Lewis J. G., Simon H. D. (1994). A shifted block Lanczos algorithm for solving sparse symmetric generalized eigenproblems. *SIAM Journal on Matrix Analysis and Applications*, 15(1), 228-272

Hilber H. M., Hughes T. J. (1978). Collocation, dissipation and [overshoot] for time integration schemes in structural dynamics. *Earthquake Engineering and Structural Dynamics*, 6(1), 99-117.

Karimi A. H., Karimi M. S., Kheyroddin A., Shahkarami A. A. (2016). Experimental and numerical study on seismic behavior of an infilled masonry wall compared to an arched masonry wall. *Structures*, 8, 144-153

Lee J., Fenves G. L. (1998). Plastic-damage model for cyclic loading of concrete structures. *Journal of engineering mechanics*, 124(8), 892-900.

Lubliner J., Oliver J., Oller S., Oñate, E. (1989). A plastic-damage model for concrete. *International Journal of solids and structures*, 25(3), 299-326.

Mortezaei A., Motaghi A. (2016). Seismic assessment of the world's tallest pure-brick tower including soil-structure interaction. *Journal of Performance of Constructed Facilities*, 30(5).

Poiani M., Gazzani V., Clementi F., Milani G., Valente M., Lenci S. (2018). Iconic crumbling of the clock tower in Amatrice after 2016 central Italy seismic sequence: advanced numerical insight. *Procedia Structural Integrity*, 11, 314-321.

Rayleigh J. (1945). *The theory of sound*. Dover, New York.

Somma F., Lignola G., Ramaglia G., de Sanctis L., Iovino M., Oztoprak S., Flora A. (2023). An interdisciplinary investigation of the seismic performance of a historic tower in Istanbul during the 1999 Kocaeli earthquake. *Bulletin of Earthquake Engineering*, 21 (5), 2921-2945.

Tiberti S., Acito M., Milani G. (2016). Comprehensive FE numerical insight into Finale Emilia Castle behavior under 2012 Emilia Romagna seismic sequence: Damage causes and seismic vulnerability mitigation hypothesis. *Engineering Structures*, 117, 397-421.

Valente M., Milani G. (2018). Effects of geometrical features on the seismic response of historical masonry towers. *Journal of Earthquake Engineering*, 22(sup1), 2-34.

Vasconcelos G., Lourenço P. B. (2009). In-plane experimental behavior of stone masonry walls under cyclic loading. *Journal of Structural Engineering*, 135(10), 1269-1277.

Vinale F., Simonelli A. L. (1983). L'eterogeneità dei terreni nei fenomeni di amplificazione locale. *Proceedings of the 15th Geotechnical National Conference*, Spoleto, Italy, 4-6.

Vucetic M., Dobry, R. (1991). Effect of Soil Plasticity on Cyclic Response. *Journal of Geotechnical Engineering*, 117 (1), 89–107.